

Supporting Information

High electrolysis performance of the SOEC cathode by creating oxygen vacancies to regulate the adsorption energy

Yongqian Du^a, Longyan Zhao^a, Yanzhi Xiao^a, Jiangrong Kong^{*,a}, Peng Liu^b,

Xianfeng Yang^b, Tao Zhou^a

^a Hunan Provincial Key Laboratory of Efficient and Clean Utilization of Manganese Resources, College of Chemistry and Chemical Engineering, Central South University, Changsha 410083, China

^b School of Materials Science and Engineering, Changsha University of Science and Technology, Changsha 410114, China

** Corresponding Author. E-mail: kongjr@csu.edu.cn Tel: +86-13548773795*

Experimental

Materials preparation

All electrode and electrolyte powder materials used in the experiment were prepared by sol-gel method. The $\text{Sr}_{1.9}\text{Fe}_{1.3}\text{Cu}_{0.2}\text{Mo}_{0.4}\text{Ti}_{0.1}\text{O}_{6-\delta}$ (SFCMT) powders were prepared by a modified Pechini method. N, N-Dimethyl formamide (DMF) was used as the solution, to which a small amount of citric acid was first added under high speed stirring, and then sequentially added tetrabutyl titanate, $\text{Sr}(\text{NO}_3)_2$, $\text{Fe}(\text{NO}_3)_3 \cdot 9\text{H}_2\text{O}$, $\text{Cu}(\text{NO}_3)_2$, and $(\text{NH}_4)_6\text{Mo}_7\text{O}_{24} \cdot 4\text{H}_2\text{O}$ in stoichiometric ratio. Then added the appropriate amount of citric acid in proportionally (metal ion: citric acid=1:2). After continuous stirring until the solution was completely mixed well. The solution was placed in a water bath at 80°C with vigorous stirring for several hours to obtain a viscous gel-like substance. The gel was subjected to drying treatment at 250°C for 4 h to remove nitrate ions and organic components and to obtain fluffy precursors. The precursors were ground to powder form and calcined in air at 1100°C for 5 h to obtain SFCMT powders. $\text{Sm}_{0.2}\text{Ce}_{0.8}\text{O}_{1.9}$ (SDC) and $\text{Gd}_{0.2}\text{Ce}_{0.8}\text{O}_{1.9}$ (GDC) were synthesized by the same method.

Characterization

The crystal structure and stability of the samples were analyzed using an X-ray diffraction (XRD, Bruker D8 Advance, Cu $K\alpha$ radiation) with diffraction angles ranging from 20 - 80° . The surface morphology of the composite cathode was observed by scanning electron microscopy (SEM, ZEISS Sigma 300) before and after reduction, as well as cross-sectional views. High-resolution transmission electron microscopy (HR-TEM, JEOL JEM-F200) was employed to analyze the lattice parameters of the composite cathode powders. Energy dispersive X-ray spectrometer (EDX, JED-2300T) was employed to analyze the composition and distribution of elements. X-ray

photoelectron spectroscopy (XPS, Thermo Scientific K-Alpha, Al K α radiation) was used to analyze the shift in elemental valence states of composite cathode powders before and after reduction. The oxygen vacancy concentration of composite cathodes was studied by thermogravimetric analysis (TGA, PerkinElmer STA 6000) and electron paramagnetic resonance (EPR, Bruker EMXplus-6/1). Infrared spectroscopy (IR, Thermo Scientific Nicolet iS20) and temperature-programmed desorption of CO₂ (CO₂-TPD, Micromeritics AutoChem II 2920) were employed to investigate the CO₂ adsorption capacity of composite cathodes.

Cell fabrication and electrochemical testing

The flow of single cell preparation in this study is shown in Figure S17. SDC powders was formed into 20 mm diameter discs as electrolyte substrate by dry-pressing method. These electrolyte discs were subsequently calcined in air for 4 h to obtain a dense structure. A GDC buffer layer was added as a barrier by screen printing to prevent possible side reactions between the electrolyte and the electrode. GDC buffer layer was sintered in air at 1400°C for 2 h. Similarly, mixing the SFCMT and GDC powders by ethanol ball-milling in a mass ratio of 7:3 and repeated the above screen-printing process. Subsequently, SFCMT-GDC cathodes with an effective area of 0.25 cm² were sintered in air at 1100°C for 2 h. Platinum paste is printed on both sides of the electrolyte as the counter electrode and reference electrode, forming a three-electrode system. The cells were tested using platinum grid as current collector and silver wire as electron conductor. The electrochemical test setup is shown in the Figure S18.

Prior to the electrolysis test, pure H₂ (50 mL min⁻¹) was passed to the fuel electrode side at 800°C for reduction treatment to obtain a Cu@SFCMT-GDC cathode. Subsequently switched to pure CO₂ atmosphere (50 mL min⁻¹) for electrochemical testing. The I-V curves during electrolysis were monitored using an electrochemical

workstation (CHI660e) with applied voltages ranging from 0 to 1.8 V. The electrochemical AC impedance was also measured with a set frequency range of 0.01 Hz-100 kHz. The raw AC impedance data were subjected to DRT analysis.

Computational details

DFT was performed as implemented in the Vienna Ab initio simulation package (VASP) in all calculations. The exchange-correlation potential is described by using the generalized gradient approximation of Perdew-Burke-Ernzerhof (GGA-PBE). The projector augmented-wave (PAW) method is employed to treat interactions between ion cores and valence electrons. The plane-wave cutoff energy was fixed to 500 eV. Given structural models were relaxed until the Hellmann–Feynman forces smaller than -0.02 eV/Å and the change in energy smaller than 10^{-5} eV was attained. The vacuum thickness was set to be 25 Å to minimize interlayer interactions. During the relaxation, the Brillouin zone was represented by a Γ centered k-point grid of $5 \times 5 \times 1$. Grimme's DFT-D3 methodology was used to describe the dispersion interactions among all the atoms in adsorption models.

Supporting figures

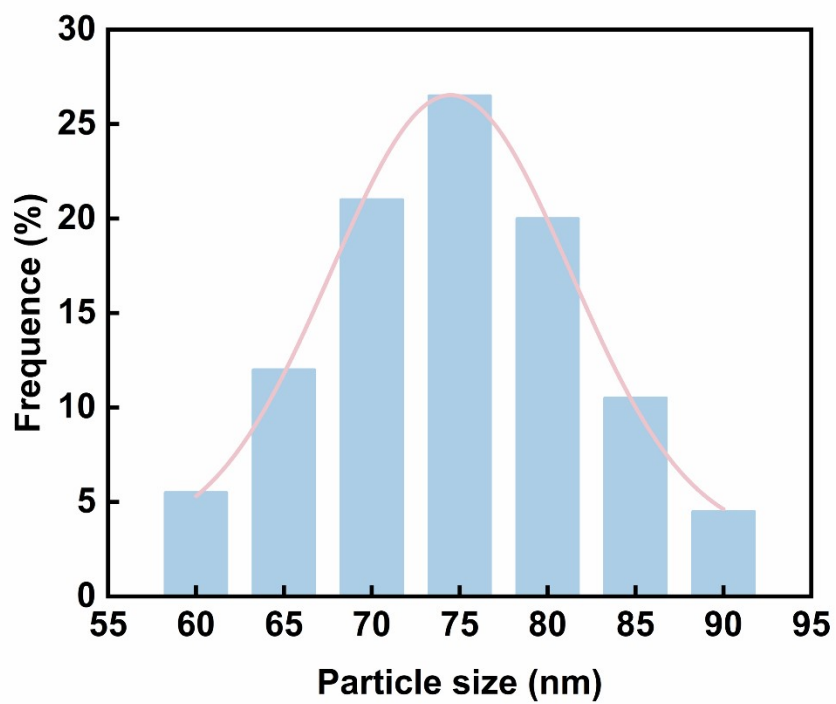


Figure S1. Particle size distribution of Cu nanoparticles.

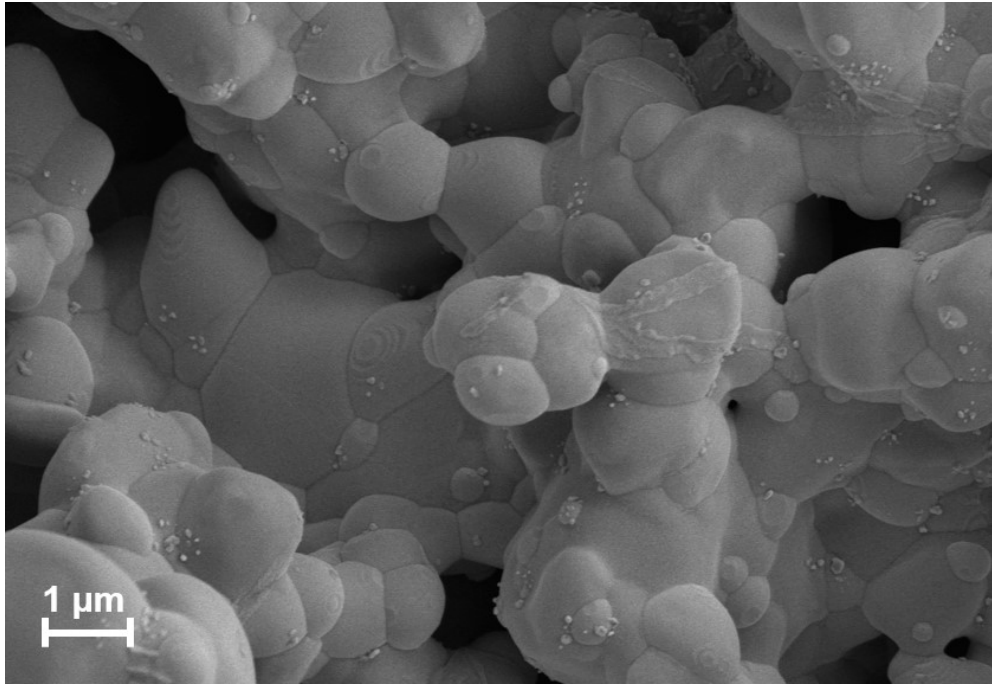


Figure S2. The morphology of Cu@SFCMT-GDC cathode reduced at 700°C.

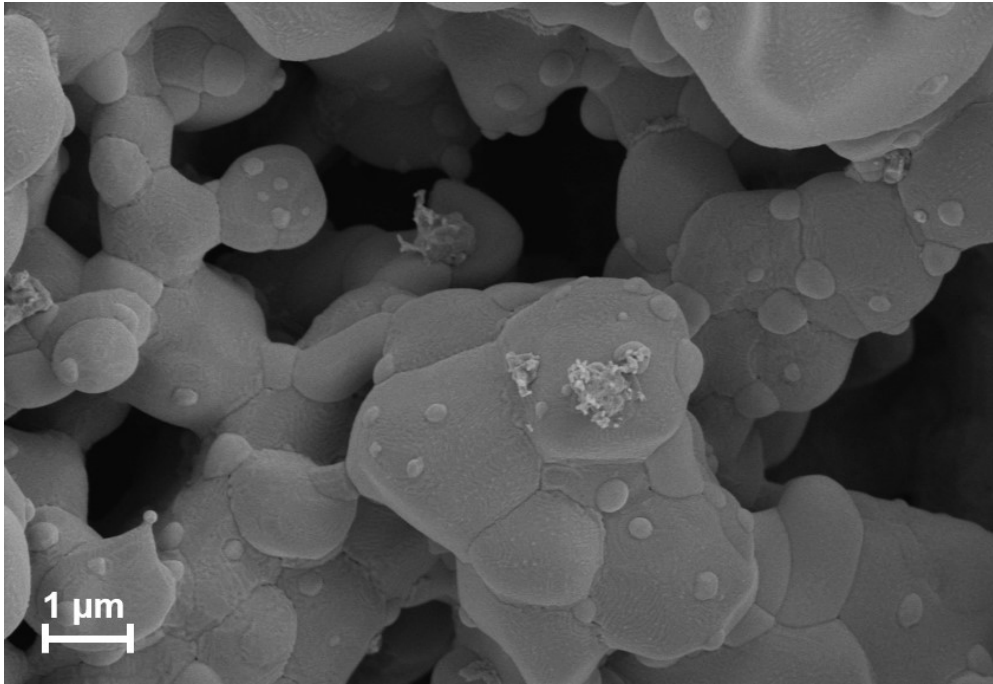


Figure S3. The morphology of Cu@SFCMT-GDC cathode reduced at 900°C.

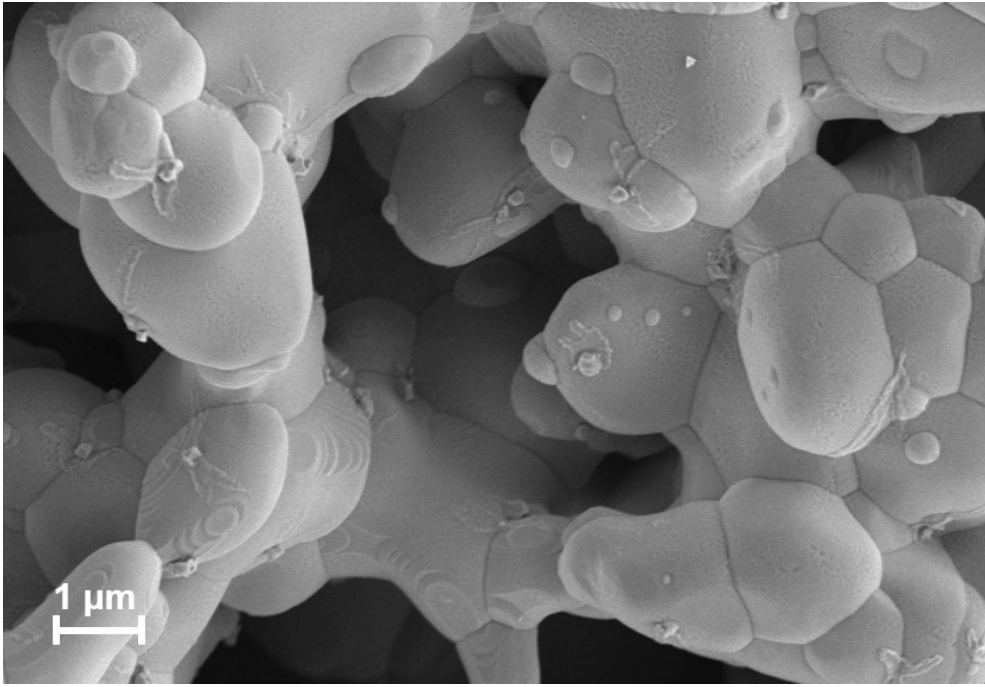


Figure S4. The morphology of Cu@SFCMT-GDC cathode reduced for 3h.

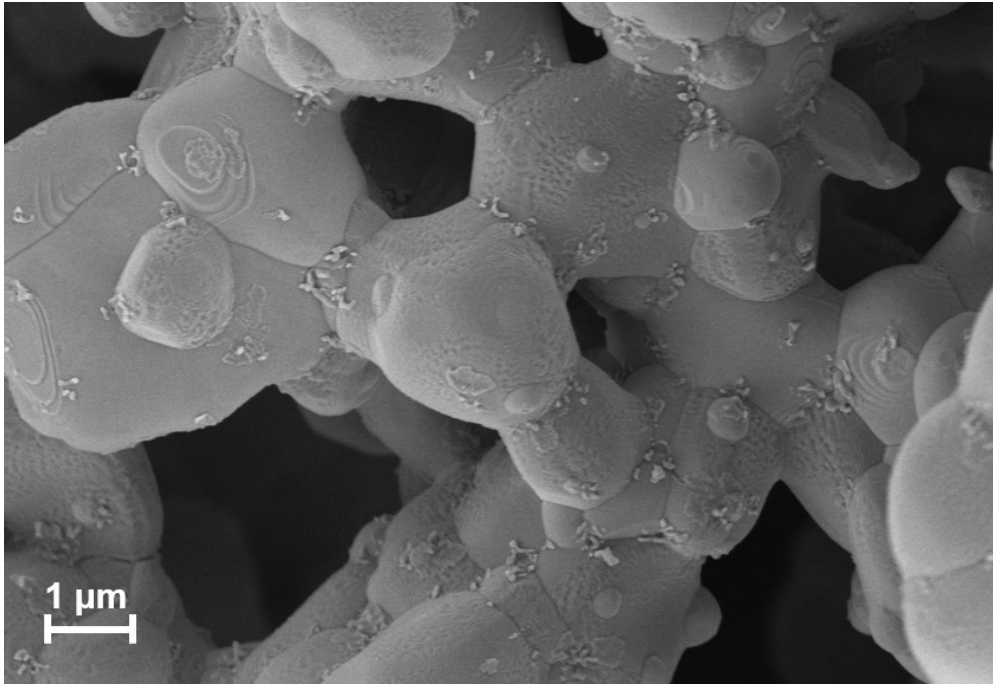


Figure S5. The morphology of Cu@SFCMT-GDC cathode reduced for 7h.

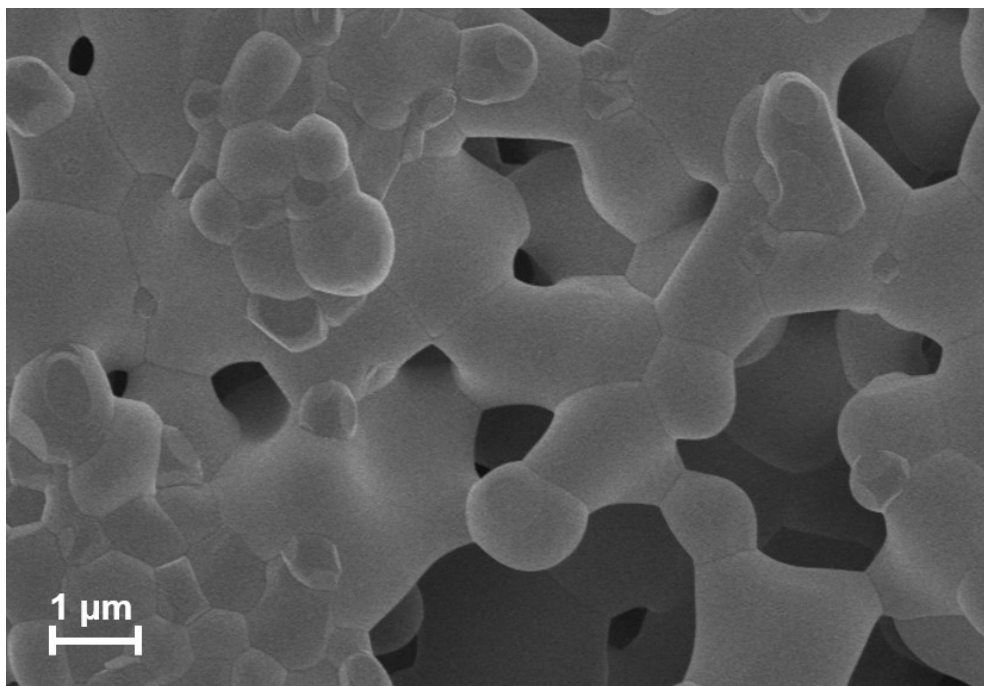


Figure S6. The morphology of Cu@SFCMT-GDC cathode reduced with $50 \text{ mL} \cdot \text{min}^{-1}$ 10% H_2/Ar flow rate.

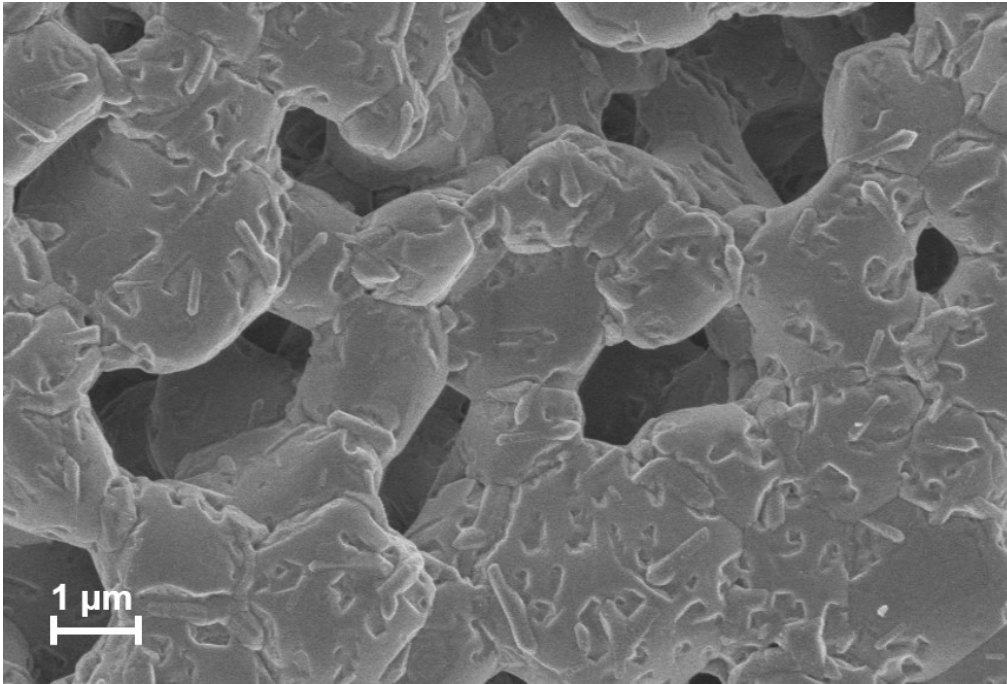


Figure S7. The morphology of Cu@SFCMT-GDC cathode reduced with $150 \text{ mL} \cdot \text{min}^{-1}$ 10% H_2/Ar flow rate.

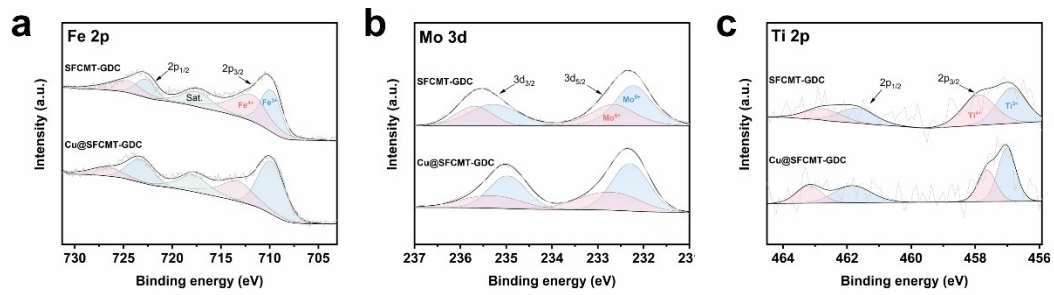


Figure S8. XPS spectra of (a) Fe 2p, (b) Mo 3d and (c) Ti 2p for SFCMT-GDC and Cu@SFCMT-GDC samples.

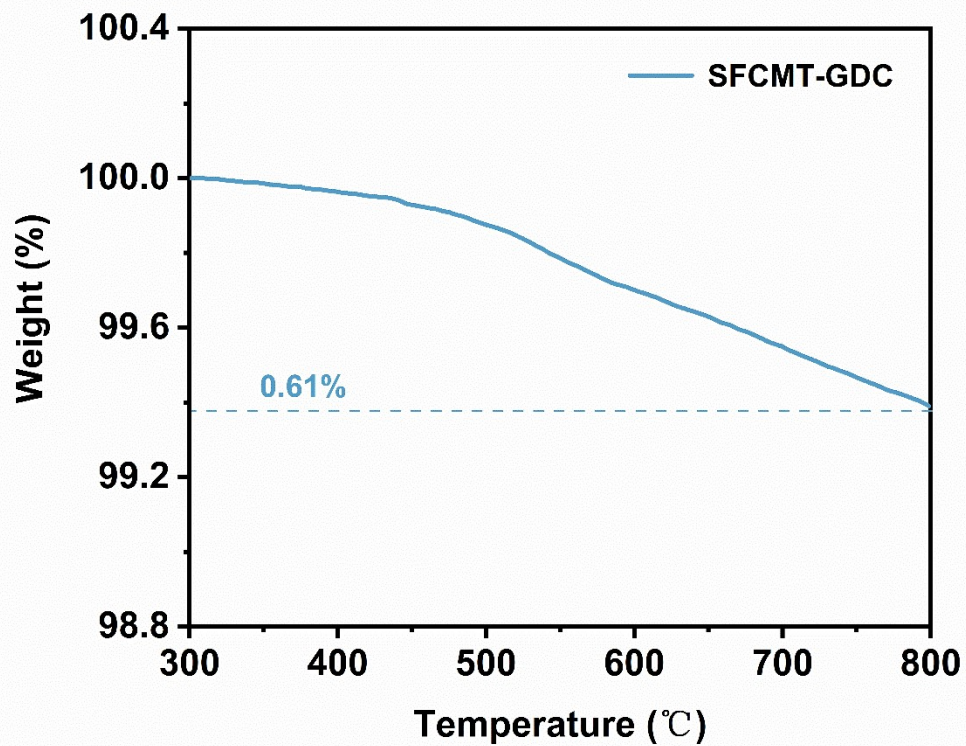


Figure S9. TGA curve of SFCMT-GDC tested in air.

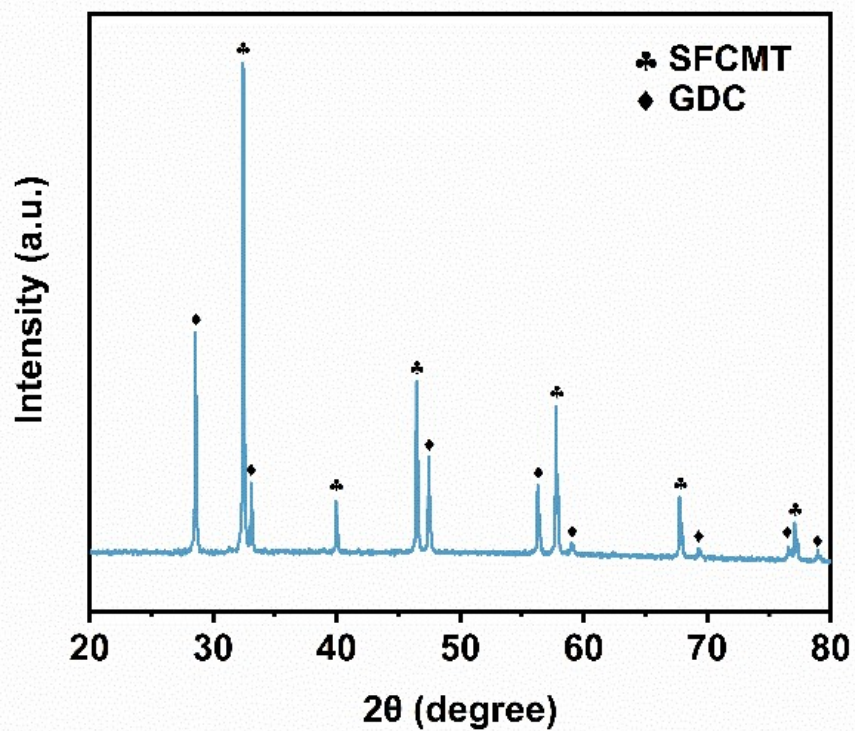


Figure S10. The XRD pattern of the SFCMT-GDC composite cathode after TGA in nitrogen atmosphere.

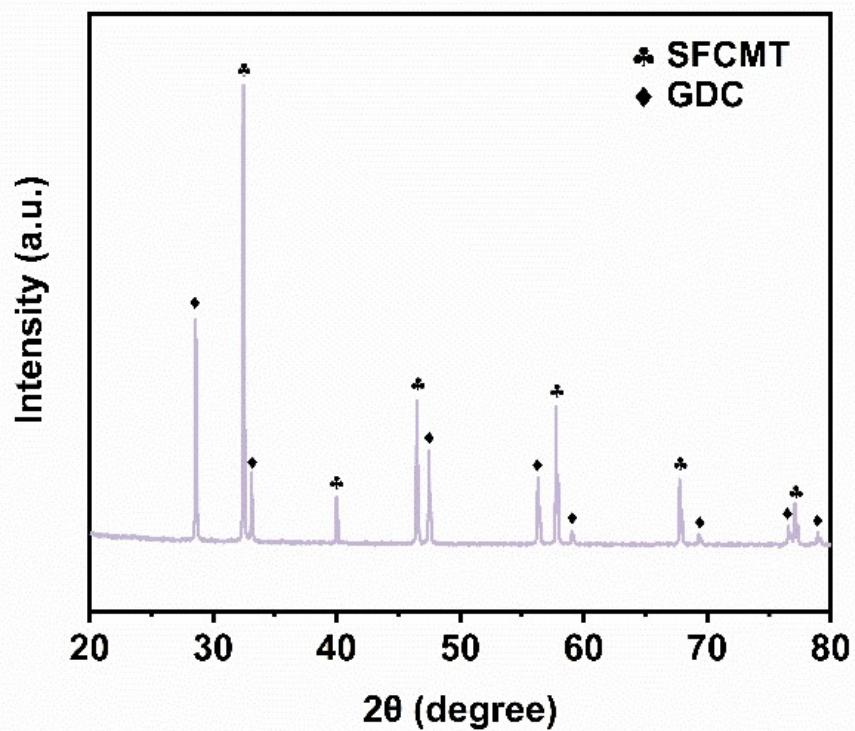


Figure S11. The XRD pattern of the SFCMT-GDC composite cathode after TGA in air atmosphere.

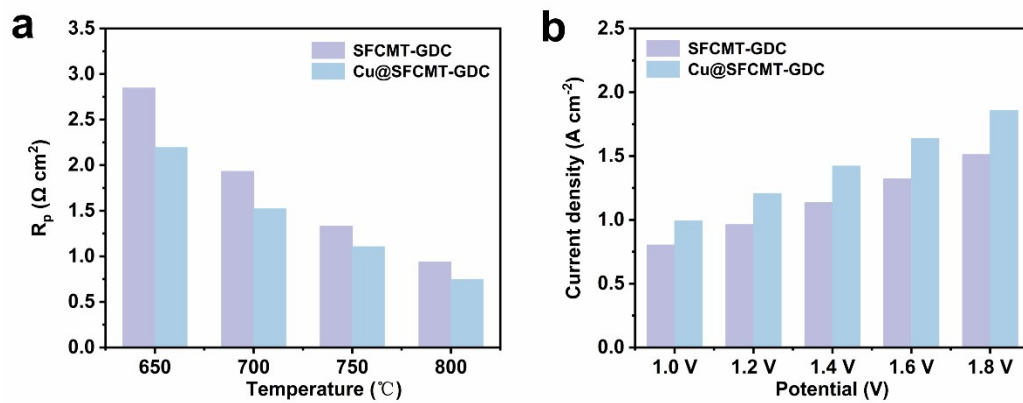


Figure S12. Comparison of (a) R_p at different temperatures and (b) current density at different applied voltages for SFCMT-GDC and Cu@SFCMT-GDC cathodes.

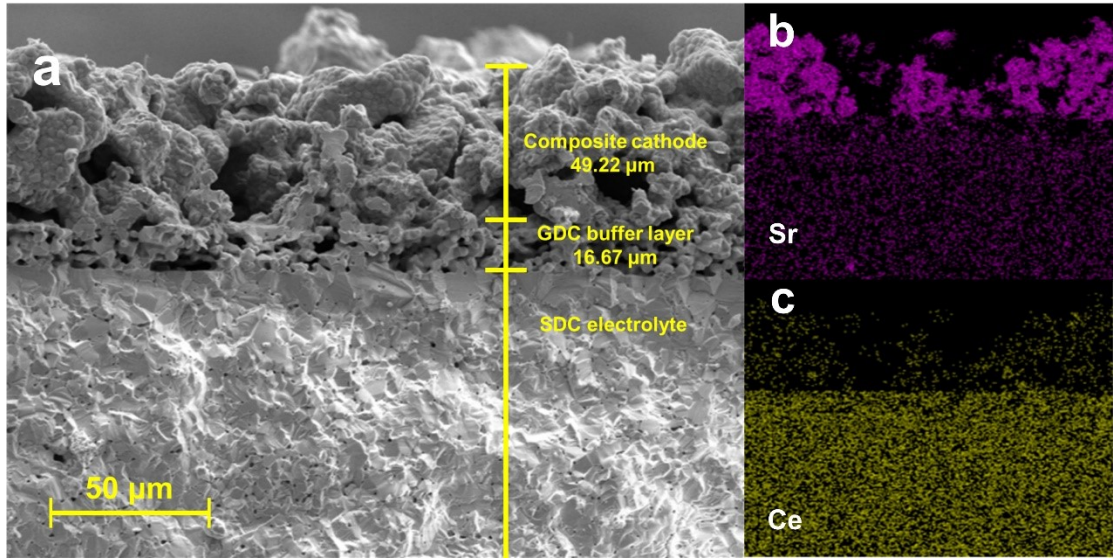


Figure S13. (a) Cross-sectional SEM image of a single cell after testing; Distribution of elements (b) Sr and (c) Ce.

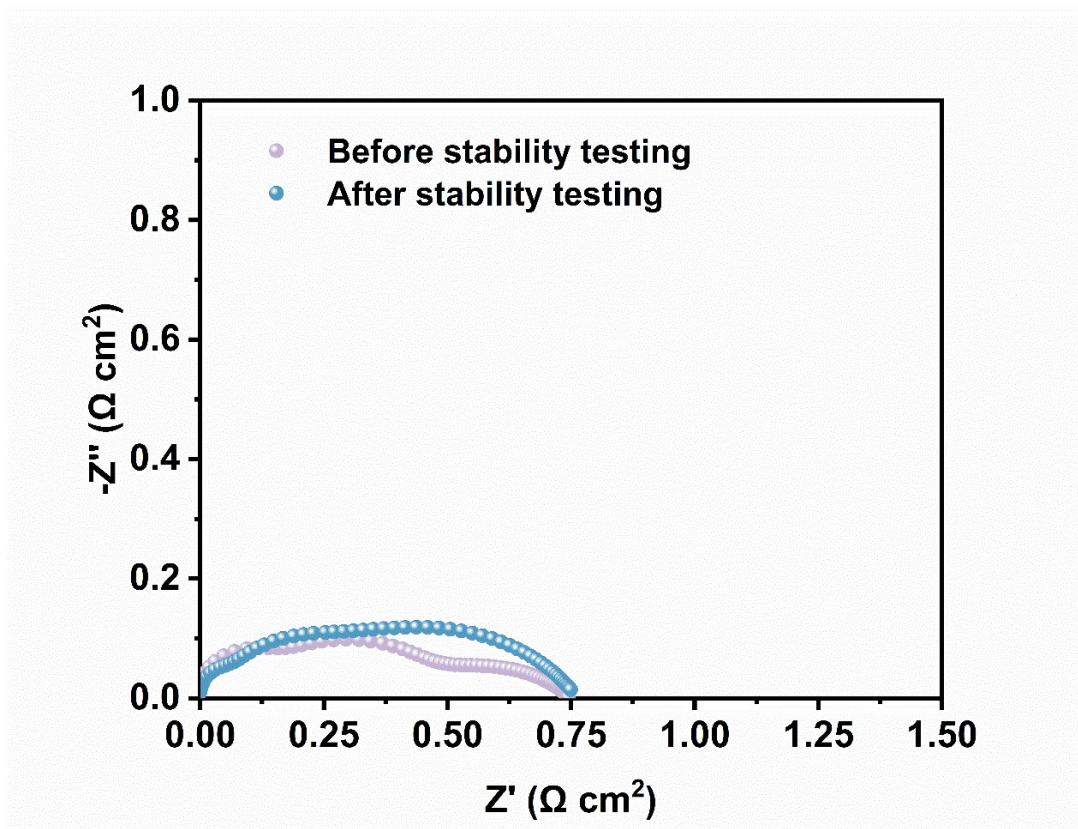


Figure S14. The comparison of the EIS of the single cells at 800°C before and after the stability test

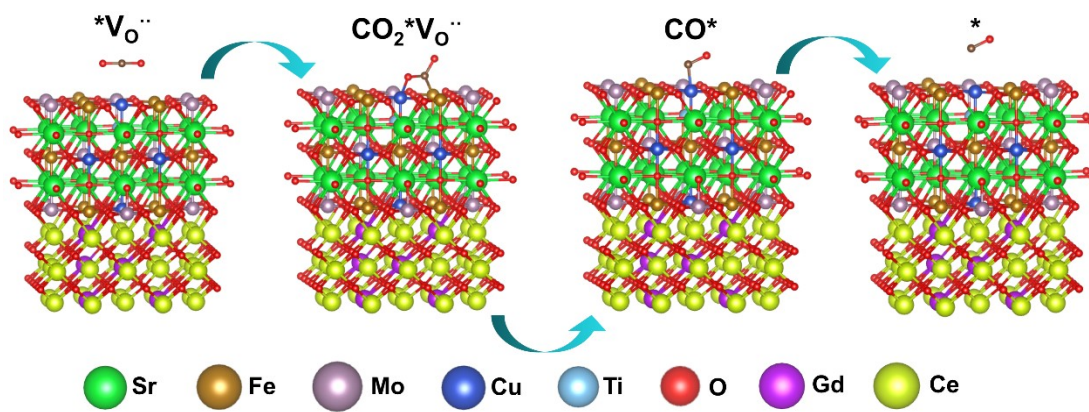


Figure S15. Adsorption configuration of reaction intermediates on the SFCMT-GDC cathode surface for CO₂RR.

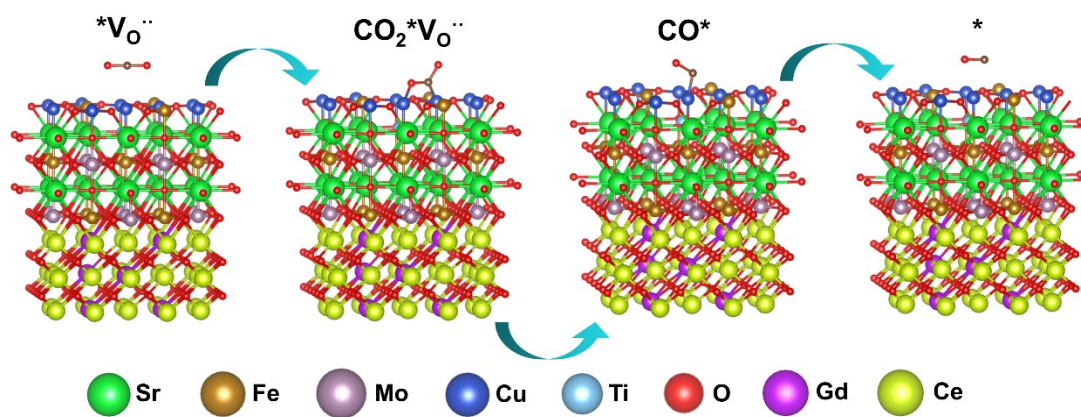


Figure S16. Adsorption configuration of reaction intermediates on the Cu@SFCMT-GDC cathode surface for CO₂RR.

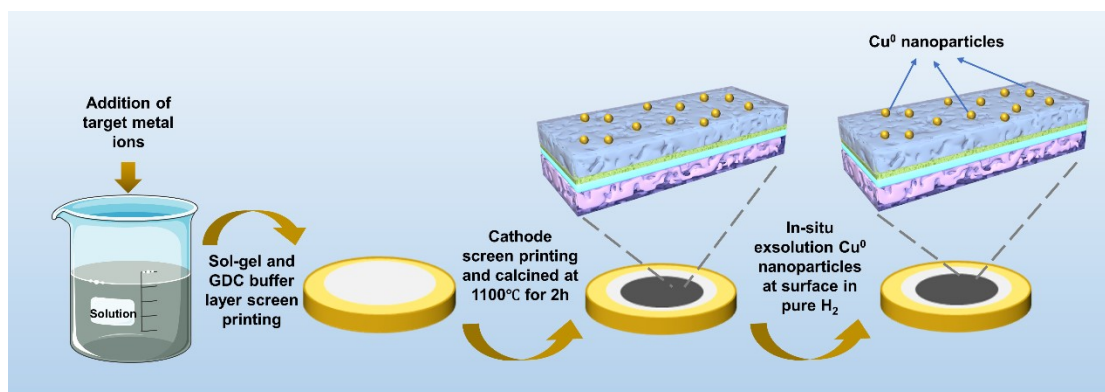


Figure S17. Schematic diagram of the preparation process of a single cell.

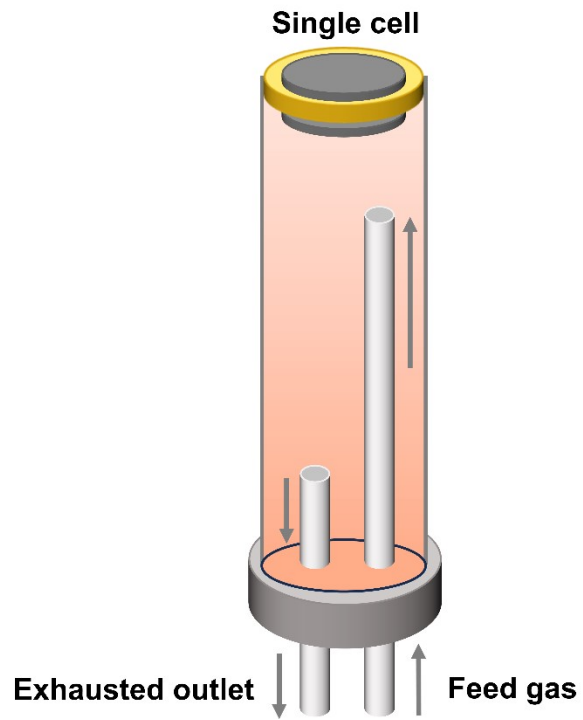


Figure S18. Home-made electrochemical test set for laboratory.

Supporting tables

Table S1. XPS analysis of Fe 2p for SFCMT-GDC samples before and after reduction.

Sample	B.E. Fe 2p/ eV		Relative atomic concentration/ %	
	Fe ³⁺	Fe ⁴⁺	Fe ³⁺	Fe ⁴⁺
SFCMT-GDC	710.19/723.68	713.35/726.14	48.75	51.25
Cu@SFCMT-GDC	710.42/723.22	713.55/726.35	62.07	37.93

Table S2. XPS analysis of Mo 3d for SFCMT-GDC samples before and after reduction.

Sample	B.E. Mo 3d/ eV		Relative atomic concentration/ %	
	Mo ⁵⁺	Mo ⁶⁺	Mo ⁵⁺	Mo ⁶⁺
SFCMT-GDC	232.22/235.27	232.67/235.69	61.23	38.77
Cu@SFCMT-GDC	231.93/235.09	232.39/235.44	61.45	38.55

Table S3. XPS analysis of Ti 2p for SFCMT-GDC samples before and after reduction.

Sample	B.E. Ti 2p/ eV		Relative atomic concentration/ %	
	Ti ³⁺	Ti ⁴⁺	Ti ³⁺	Ti ⁴⁺
SFCMT-GDC	456.87/461.69	457.88/462.75	52.96	47.04
Cu@SFCMT-GDC	457.47/462.64	458.14/464.09	61.25	38.75

Table S4. XPS analysis of O 1s for SFCMT-GDC samples before and after reduction.

Sample	B.E. O 1s/ eV			Relative atomic concentration/ %		
	O ²⁻	O ⁻ / O ₂ ²⁻	OH ⁻ /CO ₂ ^{- 3}	O ²⁻	O ⁻ / O ₂ ^{- 2}	OH ⁻ /CO ₂ ^{- 3}
SFCMT-GDC	528.42	529.09	531.19	23.43	19.43	57.14
Cu@SFCMT-GDC	528.64	529.36	531.37	14.38	20.26	65.36